MODELING AND CONTROL OF THERMOSTATICALLY CONTROLLED LOADS

Soumya Kundu
University of Michigan
Ann Arbor, USA
soumyak@umich.edu

Nikolai Sinitsyn
Los Alamos National Laboratory
Los Alamos, USA
sinitsyn@lanl.gov

Scott Backhaus
Los Alamos National Laboratory
Los Alamos, USA
backhaus@lanl.gov

Ian Hiskens
University of Michigan
Ann Arbor, USA
hiskens@umich.edu

Abstract - As the penetration of intermittent energy sources grows substantially, loads will be required to play an increasingly important role in compensating the fast time-scale fluctuations in generated power. Recent numerical modeling of thermostatically controlled loads (TCLs) has demonstrated that such load following is feasible, but analytical models that satisfactorily quantify the aggregate power consumption of a group of TCLs are desired to enable controller design. We develop such a model for the aggregate power response of a homogeneous population of TCLs to uniform variation of all TCL setpoints. A linearized model of the response is derived, and a linear quadratic regulator (LQR) has been designed. Using the TCL setpoint as the control input, the LQR enables aggregate power to track reference signals that exhibit step, ramp and sinusoidal variations.

Keywords - Load modeling; load control; renewable energy; linear quadratic regulator.

1 INTRODUCTION

GROWTH in renewable power generation brings with it concerns for grid reliability due to the intermittency and non-dispatchability associated with such sources. Conventional power generators have difficulty in manoeuvering to compensate for the variability in the power output from renewable sources. On the other hand, electrical loads offer the possibility of providing the required generation-balancing ancillary services. It is feasible for electrical loads to compensate for energy imbalance much more quickly than conventional generators, which are often constrained by physical ramp rates.

A population of thermostatically controlled loads (TCLs) is well matched to the role of load following. Research into the behavior of TCLs began with the work of [1] and [2], who proposed models to capture the hybid dynamics of each thermostat in the population. The aggregate dynamic response of such loads was investigated by [4], who derived a coupled ordinary and partial differential equation (Fokker-Planck equation) model. The model was derived by first assuming a homogeneous group of thermostats (all thermostats having the same parameters), and then extended using perturbation analysis to obtain the model for a non-homogeneous group of thermostats. In [5], a discrete-time model of the dynamics of the temperatures of individual thermostats was derived, assuming no external random influence. That work was later extended by [6] to introduce random influences and heterogeneity.

Although the traditional focus has been on direct load control methods that directly interrupt power to all loads, recent work in [3] proposed hysteresis-based control by manipulating the thermostat setpoint of all loads in the population with a common signal. While it is difficult to keep track of the temperature and power demands of individual loads in the population, the probability of each load being in a given state (ON - drawing power or OFF - not drawing any power) can be estimated rather accurately. System identification techniques were used in [3] to obtain an aggregate linear TCL model, which was then employed in a minimum variance control law to demonstrate the load following capability of a population of TCLs.

In this paper, we derive a transfer function relating the aggregate response of a homogeneous group of TCLs to disturbances that are applied uniformly to the thermostat setpoints of all TCLs. We start from the hybrid temperature dynamics of individual thermostats in the population, and derive the steady-state probability density functions of loads being in the ON or OFF states. Using these probabilities we calculate aggregate power response to a setpoint change. We linearize the response and design a linear quadratic regulator to achieve reference tracking by the aggregate power demand.

2 STEADY STATE DISTRIBUTION OF LOADS

2.1 Model development

The dynamic behavior of the temperature $\theta(t)$ of a thermostatically controlled cooling-load (TCL), in the ON and OFF state and in the absence of noise, can be modeled by [5],

$$\dot{\theta} = \begin{cases} -\frac{1}{CR}\left(\theta - \theta_{amb} + PR\right), & \text{ON state} \\ -\frac{1}{CR}\left(\theta - \theta_{amb}\right), & \text{OFF state} \end{cases} \tag{1}$$

where θ_{amb} is the ambient temperature, C is the thermal capacitance, R is the thermal resistance, and P is the power drawn by the TCL when in the ON state. This response is shown in Figure 1.

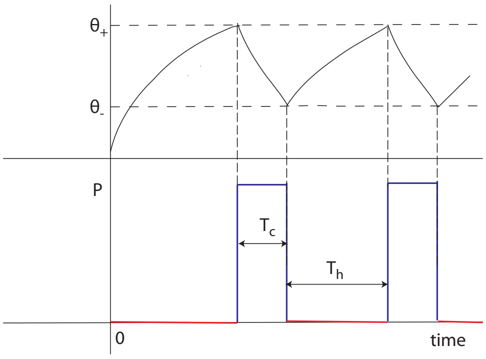

Figure 1: Dynamics of temperature of a thermostatic load.

In steady state the cooling period drives a load from temperature θ_+ to temperature θ_-. Thus solving (1) with initial condition $\theta(0) = \theta_+$ gives

$$\theta(t) \;=\; (\theta_{amb} - PR)\left(1 - e^{-\frac{t}{CR}}\right) + \theta_+ e^{-\frac{t}{CR}}. \quad (2)$$

From (2) we can calculate the steady state cooling time T_c by equating $\theta(T_c)$ to θ_-,

$$T_c = CR \ln\left(\frac{PR + \theta_+ - \theta_{amb}}{PR + \theta_- - \theta_{amb}}\right). \quad (3)$$

A similar calculation for the heating time gives,

$$T_h = CR \ln\left(\frac{\theta_{amb} - \theta_-}{\theta_{amb} - \theta_+}\right). \quad (4)$$

In general, the expressions for the times $t_c(\theta_f)$ and $t_h(\theta_f)$ taken to reach some intermediate temperature θ_f during the cooling and heating periods, respectively, are,

$$t_c(\theta_f) = CR \ln\left(\frac{PR + \theta_+ - \theta_{amb}}{PR + \theta_f - \theta_{amb}}\right) \quad (5)$$

$$t_h(\theta_f) = CR \ln\left(\frac{\theta_{amb} - \theta_-}{\theta_{amb} - \theta_f}\right). \quad (6)$$

It follows immediately that $t_c(\theta_-) = T_c$ and $t_h(\theta_+) = T_h$.

For a homogeneous[1] set of TCLs in steady state, the number of loads in the ON and OFF states, N_c and N_h respectively, will be proportional to their respective cooling and heating time periods T_c and T_h. In the absence of any appreciable noise, which ensures that all the loads are within the temperature deadband, $N_h + N_c = N$, we obtain,

$$N_c = \frac{T_c}{T_c + T_h} N \quad (7)$$

$$N_h = \frac{T_h}{T_c + T_h} N \quad (8)$$

By analogy, it follows that the number of ON-loads within a temperature band $[\theta,\ \theta_+]$ is proportional to the time taken $t_c(\theta)$ to cool a load down from θ_+ to $\theta \geq \theta_-$, and is given by

$$\begin{aligned} n_c(\theta) &= t_c(\theta)\frac{N_c}{T_c} \\ &= t_c(\theta)\frac{N}{T_c + T_h}, \end{aligned} \quad (9)$$

[1] All loads share the same values for parameters θ_{amb}, C, R and P.

where (7) was used to obtain (9). Likewise, the number of OFF-loads with temperature in the band $[\theta_-,\ \theta]$ is given by

$$n_h(\theta) = t_h(\theta)\frac{N}{T_c + T_h} \quad (10)$$

where $t_h(\theta)$ is the time taken for a load's temperature to rise from θ_- to $\theta \leq \theta_+$.

We will denote the ON probability density function by $f_1(\theta)$ and the OFF probability density function by $f_0(\theta)$, while the corresponding cumulative distribution functions are denoted $F_1(\theta)$ and $F_0(\theta)$, respectively. Because $F_0(\theta)$ is the probability of a load being in the OFF state, with temperature in the range $[\theta_-,\ \theta]$, we obtain directly that $F_0(\theta) = n_h(\theta)/N$. In establishing the equivalent relationship between $F_1(\theta)$ and $n_c(\theta)$, we must keep in mind that $F_1(\theta)$ is defined relative to the temperature band $[\theta_-,\ \theta]$, whereas $n_c(\theta)$ refers to the band $[\theta,\ \theta_+]$. Consequently, we obtain $F_1(\theta) = (N_c - n_c(\theta))/N$.

We can therefore write,

$$\begin{aligned} f_0(\theta) &= \frac{dF_0(\theta)}{d\theta} = \frac{d}{d\theta}\left(\frac{n_h(\theta)}{N}\right) \\ &= \frac{1}{N}\frac{dt_h(\theta)}{d\theta}\frac{N}{T_c + T_h} \\ &= \frac{1}{T_c + T_h}\frac{dt_h(\theta)}{d\theta} \\ &= \frac{CR}{(T_c + T_h)(\theta_{amb} - \theta)} \end{aligned} \quad (11)$$

and

$$\begin{aligned} f_1(\theta) &= \frac{dF_1(\theta)}{d\theta} = \frac{d}{d\theta}\left(\frac{N_c - n_c(\theta)}{N}\right) \\ &= \frac{CR}{(T_c + T_h)(PR + \theta - \theta_{amb})}. \end{aligned} \quad (12)$$

2.2 *Simulation*

Figure 2 shows a comparison of the densities calculated using (11) and (12) and those computed from actual simulation of the dynamics of a population of 10,000 TCLs that included a small amount of noise. The result suggests that the assumptions underlying (11) and (12) are realistic.

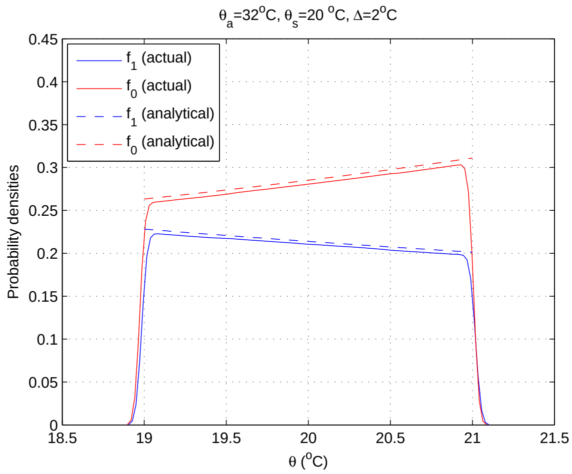

Figure 2: Steady state densities.

3 SETPOINT VARIATION

Control of active power can be achieved by making a uniform adjustment to the temperature setpoint of all loads within a large population [3]. It is assumed that the temperature deadband moves in unison with the setpoint. Figure 3 shows the change in the aggregate power consumption of a population of TCLs for a small step change in the setpoint of all devices. The resulting transient variations in the OFF-state and ON-state distributions for the population are shown in Figure 4.

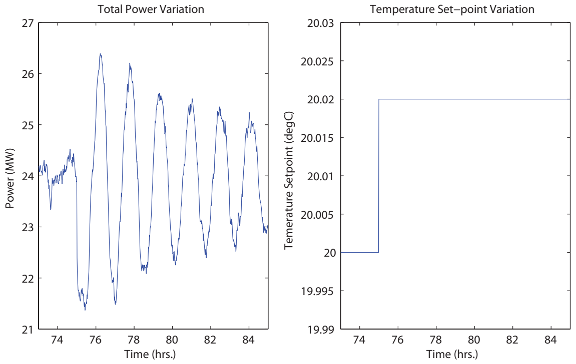

Figure 3: Change in aggregate power consumption due to a step change in temperature setpoint.

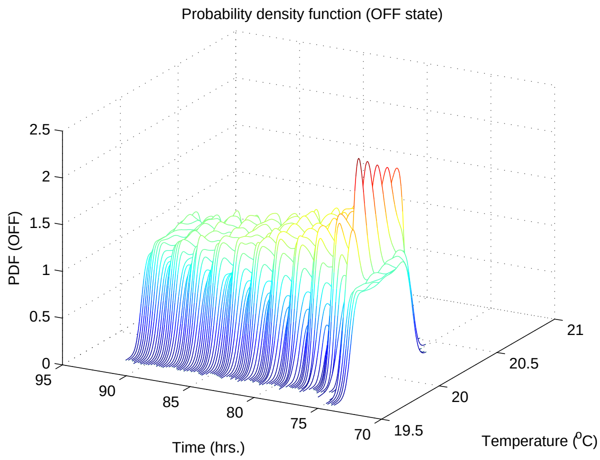

(a) OFF-state distribution.

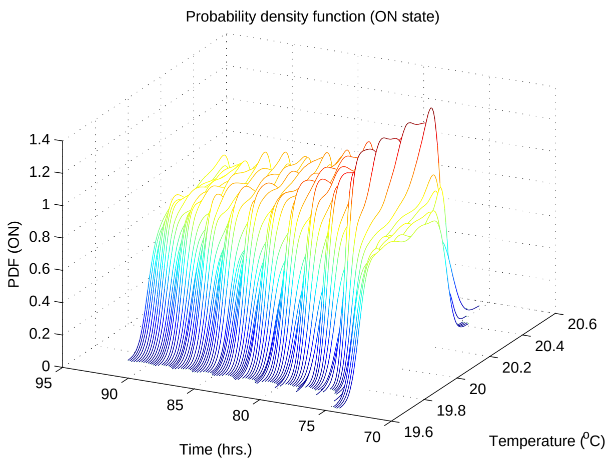

(b) ON-state distribution.

Figure 4: Variation in distribution of loads due to setpoint disturbance.

The aggregate power consumption at any instant in time is proportional to the number of loads in the ON state at that instant. The first step in quantifying the change in power due to a step change in setpoint is therefore to analyze the behavior of the TCL probability distributions. Figure 5 depicts a situation where the setpoint has just been increased. The original deadband ranged from θ_-^0 to θ_+^0, with the setpoint at $(\theta_-^0 + \theta_+^0)/2$. After the positive step change, the new deadband lies between θ_- to θ_+, with the deadband width $\Delta = \theta_+^0 - \theta_-^0 = \theta_+ - \theta_-$ remaining unchanged. The setpoint is shifted by $\delta = \theta_- - \theta_-^0 = \theta_+ - \theta_+^0$. To solve for the power consumption, we need to consider four different TCL starting conditions immediately after the step change in setpoint, i.e. a-d in Figure 5. Using Laplace transforms, we compute the time dependence of the power consumption for each of these loads (shown in Figure 6) and then compute the total power consumption by integrating over the distributions f_0 and f_1. At the instant the step change in applied, the temperatures of loads at points a, b, c and d are θ_a, θ_b, θ_c and θ_d, respectively.

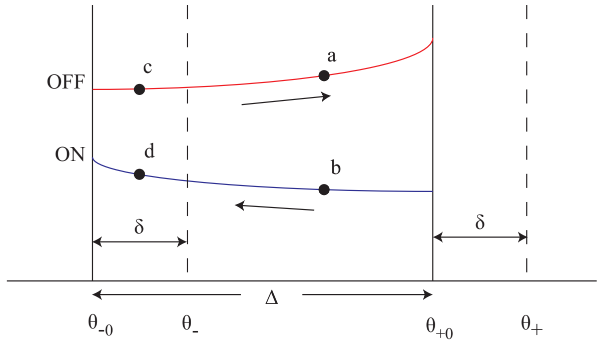

Figure 5: Different points of interest on the density curves.

The power consumption $g_a(t, \tau_a)$ of the load at a starting from the instant when the step change in setpoint is applied is shown in Figure 6(a). All the loads in the OFF-state and having a temperature between θ_- and θ_+^0 at the instant when the deadband shift occurs will have power waveforms similar in nature to $g_a(t, \tau_a)$. Thus the load at a typifies the behavior of all the loads lying on the OFF-state density curve between θ_- and θ_+^0. The same argument applies for loads at points b, c and d. Figures 6(a)-6(d) illustrate the general nature of the power waveforms of the loads in all four regions, marked by a, b, c and d in Figure 5.

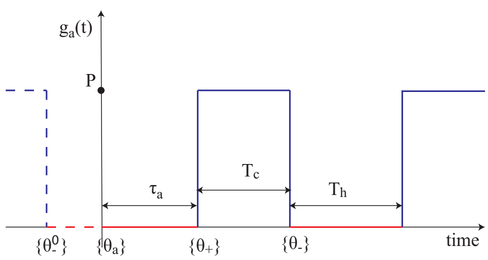

(a) Power waveform at point a.

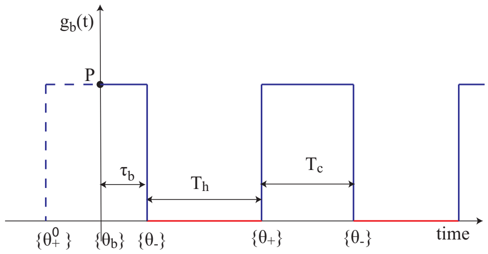

(b) Power waveform at point b.

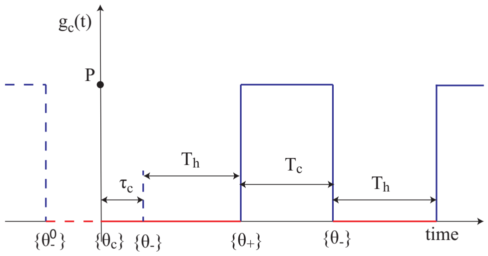

(c) Power waveform at point c.

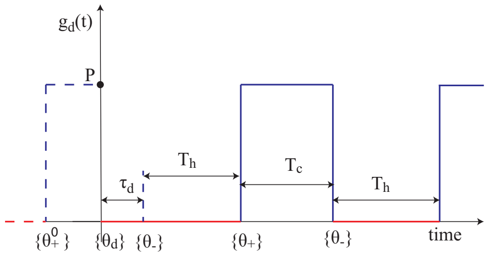

(d) Power waveform at point d.

Figure 6: Power waveforms at four different points marked in Figure 5.

It is shown in the appendix that the Laplace transform of $g_a(t, \tau_a)$ is given by

$$\mathbf{G}_a(s, \tau_a) = e^{-s\tau_a}\mathbf{G}(s)$$

where

$$\mathbf{G}(s) = \frac{P(1 - e^{-sT_c})}{s(1 - e^{-s(T_c+T_h)})}$$

and $\tau_a = T_h - t_h(\theta_a)$, with $t_h(\theta_a)$ given by (6). Averaging over all such loads (represented by a) on the OFF density curve between temperatures θ_- and θ_+^0, we obtain the Laplace transform of the average power demand,

$$\mathbf{P}_a(s) = \int_{\theta_-}^{\theta_+^0} f_0(\theta_a)\mathbf{G}_a(s, \tau_a)d\theta_a \qquad (13)$$

where $f_0(\theta_a)$ can be computed from (11).

In Figure 6(b), a load at point b on the ON density curve in Figure 5 has power consumption $g_b(t, \tau_b)$, where $\tau_b = T_c - t_c(\theta_b)$, and $t_c(\theta_b)$ is given by (5). The Laplace transform is derived in the appendix as

$$\mathbf{G}_b(s, \tau_b) = \Big(e^{s(T_c-\tau_b)}\mathbf{G}(s) - \frac{P}{s}\big(e^{s(T_c-\tau_b)} - 1\big)\Big).$$

We can compute the average power demand of all the loads represented by b as

$$\mathbf{P}_b(s) = \int_{\theta_-}^{\theta_+^0} f_1(\theta_b)\mathbf{G}_b(s, \tau_b)d\theta_b. \qquad (14)$$

In Figure 6(c), the power consumption $g_c(t, \tau_c)$ of a load at point c on the OFF density curve in Figure 5 has the Laplace transform

$$\mathbf{G}_c(s, \tau_c) = e^{-s(T_h+\tau_c)}\mathbf{G}(s),$$

where $\tau_c = CR\ln\left(\frac{\theta_{amb}-\theta_-}{\theta_{amb}-\theta_c}\right)$. The average power demand of the loads represented by the point c is then given by

$$\mathbf{P}_c(s) = \int_{\theta_-^0}^{\theta_-} f_0(\theta_c)\mathbf{G}_c(s, \tau_c)d\theta_c \qquad (15)$$

Figure 6(d) depicts the situation of a load at point d on the ON density curve, that suddenly switches to the OFF state as the deadband is shifted (for now we assume the deadband is shifted to the right, i.e., there is an increase in the setpoint). The power consumption $g_d(t)$ has the Laplace transform

$$\mathbf{G}_d(s, \tau_d) = e^{-s(T_h+\tau_d)}\mathbf{G}(s),$$

where the dynamics in (1) can be solved for $\tau_d = CR\ln\left(\frac{\theta_{amb}-\theta_d}{\theta_{amb}-\theta_-}\right)$. The average power demand of the loads characterized by point d in Figure 5 is then given by

$$\mathbf{P}_d(s) = \int_{\theta_-^0}^{\theta_-} f_1(\theta_d)\mathbf{G}_d(s, \tau_d)d\theta_d. \qquad (16)$$

The average power demand of the whole population becomes,

$$\mathbf{P}_{avg}(s) = \mathbf{P}_a(s) + \mathbf{P}_b(s) + \mathbf{P}_c(s) + \mathbf{P}_d(s). \qquad (17)$$

Using (13), (14), (15) and (16) we obtain an expression for $\mathbf{P}_{avg}(s)$ that is rather complex. It is hard, and perhaps even impossible, to obtain the inverse Laplace transform. However, with the assistance of MATHEMATICA®, $\mathbf{P}_{avg}(s)$ may be expanded as a series in s. We also make use of the assumptions,

$$\Delta \ll (\theta_s - \theta_{amb} + PR)$$
$$\Delta \ll (\theta_{amb} - \theta_s)$$
$$\delta \ll \Delta$$

where θ_s is the setpoint temperature. Note that the first two assumptions require that the deadband width is small, while the third assumption requires that the shift in the deadband is small relative to the deadband width. This latter assumption ensures that the load densities are not perturbed far from their steady-state forms. Accordingly, the steady-state power consumption is given by

$$P_{avg,ss} \approx \frac{(\theta_{amb} - \theta_+)N}{\eta R},$$

where η is the electrical efficiency of the cooling equipment and N is the population size. The deviation in power response can be approximated by

$$\mathbf{P}_{tot}(s) \approx -\left(\frac{d}{s} + \frac{\omega A_\Delta}{s^2 + \omega^2}\right)\delta \qquad (18)$$

where

$$A_\Delta = \frac{5\sqrt{15}C(\theta_{amb}-\theta_+)(PR-\theta_{amb}+\theta_+)}{\eta\big(P^2R^2+3PR(\theta_{amb}-\theta_+)-3(\theta_{amb}-\theta_+)^2\big)^{3/2}} \times \frac{(3PR-\theta_{amb}+\theta_+)N}{(T_{c0}+T_{h0})},$$

$$\omega = \frac{2\sqrt{15}(\theta_{amb}-\theta_+)(PR-\theta_{amb}+\theta_+)}{CR\Delta\sqrt{P^2R^2+3PR(\theta_{amb}-\theta_+)-3(\theta_{amb}-\theta_+)^2}},$$

$$d = \frac{N}{\eta R}.$$

and T_{c0} and T_{h0} are the original (prior to the setpoint shift) steady-state cooling and heating times, respectively, given by (3) and (4). The transfer function for this linear model is,

$$\mathbf{T}(s) = \frac{\mathbf{P}_{tot}(s)}{\delta/s} = -\Big(d + \frac{A_\Delta \omega s}{s^2+\omega^2}\Big).$$

Due to the assumptions of low-noise and homogeneity, our analytical model is undamped. The actual system, on the other hand, experiences both heterogeneity and noise, and therefore will exhibit a damped response. In order to capture that effect, we have chosen to add a damping term σ (to be estimated on-line) into the model, giving

$$\mathbf{T}(s) = -\Big(d + \frac{s\omega A_\Delta}{(s+\sigma)^2+\omega^2}\Big). \qquad (19)$$

Figure 7 shows a comparison between the response calculated from the model (19) and the true response to a step change in the setpoint obtained from simulation. A damping coefficient of 0.002 min^{-1} was added, as that value gave a close match to the decay in the actual system response.

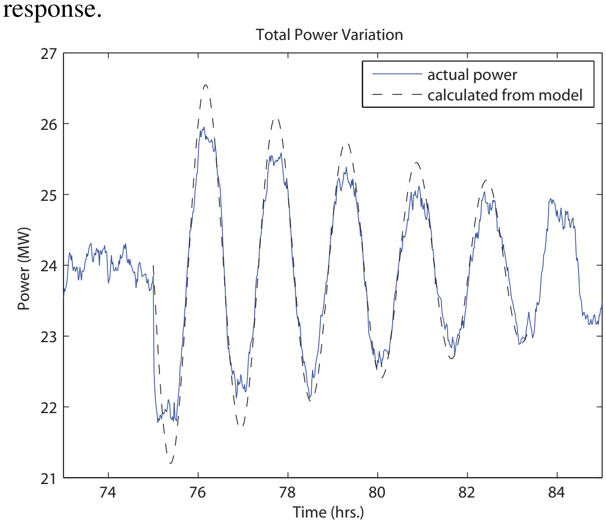

Figure 7: Comparison of the approximate model with the actual simulation, for the same setpoint disturbance as in Figure 3.

4 CONTROL LAW

The TCL load controller, described by the transfer function (19), can also be expressed in state-space form,

$$\dot{x} = \mathbf{A}x + \mathbf{B}u$$
$$y = \mathbf{C}x + \mathbf{D}u$$

where the input $u(t)$ is the shift in the deadband of all TCLs, and the output $y(t)$ is the change in the total power demand from the steady-state value. The state-space matrices are given by

$$\mathbf{A} = \begin{bmatrix} -2\sigma & -\omega \\ \frac{\sigma^2+\omega^2}{\omega} & 0 \end{bmatrix}, \qquad \mathbf{B} = \begin{bmatrix} \omega A_\Delta \\ 0 \end{bmatrix},$$
$$\mathbf{C} = \begin{bmatrix} -1 & 0 \end{bmatrix}, \qquad \mathbf{D} = -d.$$

Our goal is to design a controller using the linear quadratic regulator (LQR) approach [7] to track an exogenous reference y_d. We observe that the system has an open-loop zero very close to the imaginary axis ($d \ll \omega A_\Delta$) and hence we need to use an integral controller. Considering the integral of the output error $e = (y - y_d)$, where y_d is the reference, as the third state $w(t) = \int_0^t (y(\tau) - y_d(\tau))d\tau$ of the system, the modified state-space model becomes

$$\dot{\underline{x}} = \underline{\mathbf{A}}\,\underline{x} + \underline{\mathbf{B}}u + \mathbf{E}\,y_d$$
$$y = \underline{\mathbf{C}}\,\underline{x} + \underline{\mathbf{D}}u$$

where $\underline{x} = [x \quad w]^\top$ and,

$$\underline{\mathbf{A}} = \begin{bmatrix} \mathbf{A} & \mathbf{0}_{2\times1} \\ \mathbf{C} & 0 \end{bmatrix}, \qquad \underline{\mathbf{B}} = \begin{bmatrix} \mathbf{B} \\ \mathbf{D} \end{bmatrix},$$
$$\underline{\mathbf{C}} = \begin{bmatrix} \mathbf{C} & 0 \end{bmatrix}, \qquad \underline{\mathbf{D}} = \mathbf{D}, \quad \mathbf{E} = \begin{bmatrix} \mathbf{0}_{2\times1} \\ -1 \end{bmatrix}.$$

Minimizing the cost function

$$J = \int_0^\infty \big(\underline{x}(t)^\top Q \underline{x}(t) + u(t)^2 R\big) dt$$

where $Q \geq \mathbf{0}_{3\times3}$ and $R > 0$ are design variables, we obtain the optimal control law $u(t)$ of the form

$$u = -(\mathbf{K}\,\underline{x} + \mathbf{G}\,y_d),$$

with $\mathbf{G}$ a pre-compensator gain chosen to ensure unity DC gain. Since we can only measure the output $y(t)$ and the third state $w(t)$, the other two states are estimated using a linear quadratic estimator [7] which has the state-space form,

$$\dot{\hat{x}} = \mathbf{A}\,\hat{x} + \mathbf{B}u + \mathbf{L}(y - y_d)$$
$$\hat{y} = \mathbf{C}\,\hat{x} + \mathbf{D}u$$
$$u = -\mathbf{K}\begin{bmatrix} \hat{x} \\ w \end{bmatrix} + \mathbf{G}\,y_d.$$

The plots in Figure 8 show that the controller can be used to force the aggregate power demand of the TCL population to track a range of reference signals. The transient variations in the ON-state and OFF-state populations are shown in Figure 9. In comparison with the uncontrolled response of Figure 4, it can be seen that the controller suppresses the lengthy oscillations. Figure 9 shows that in presence of the controller, the distribution of loads *almost* always remains close to steady state, justifying an assumption made during the derivation of the model.

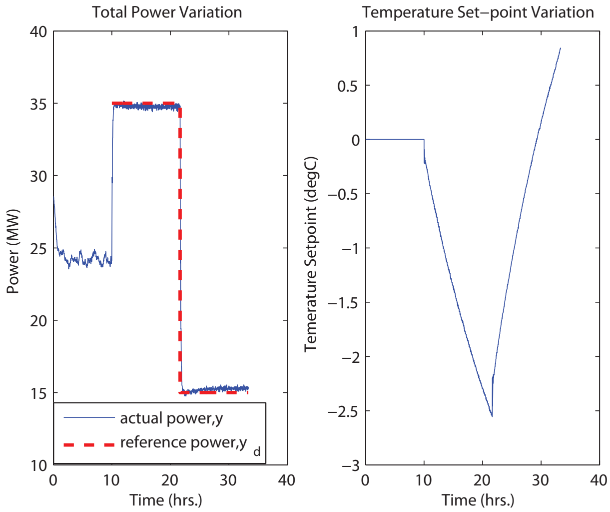

(a) Response to step reference and the control input.

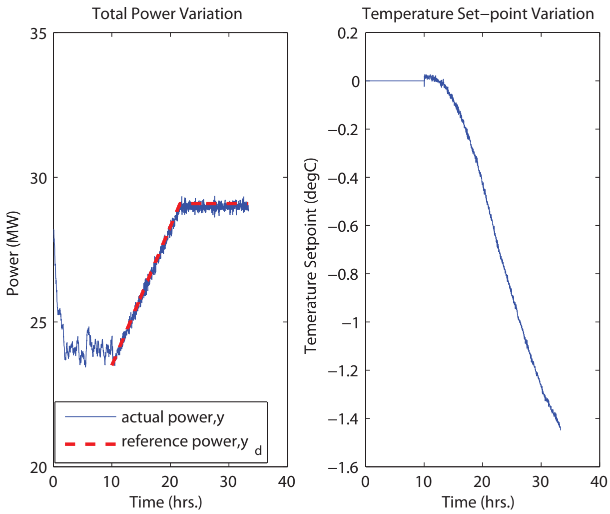

(b) Response to ramp reference and the control input.

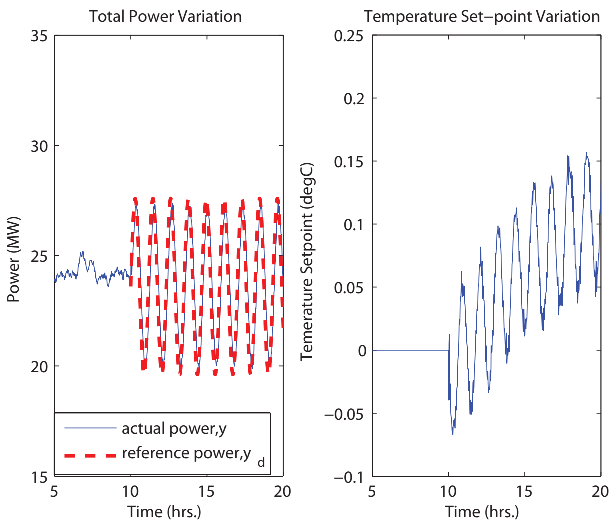

(c) Response to sinusoidal reference and the control input.

Figure 8: Reference tracking achieved through setpoint shift.

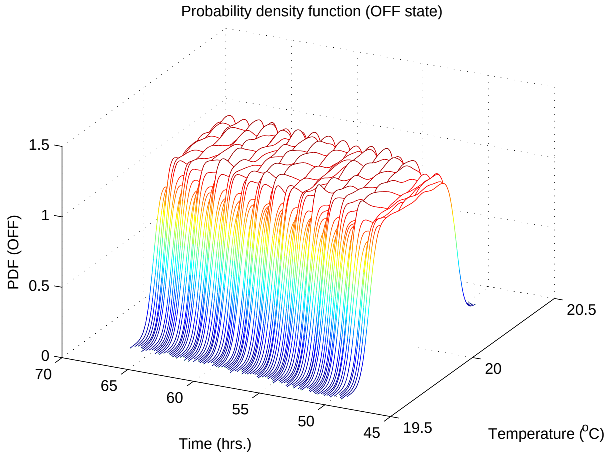

(a) OFF-state distribution.

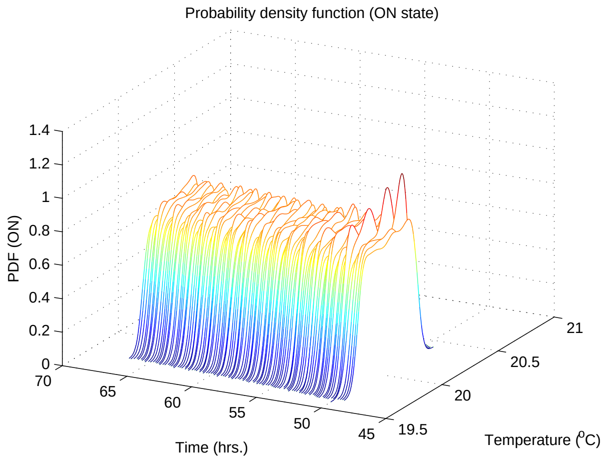

(b) ON-state distribution.

Figure 9: Variation in distribution of loads under the influence of the controller.

5 CONCLUSION

In this paper we have analytically derived a transfer function relating the change in aggregate power demand of a population of TCLs to a change in thermostat setpoint applied to all TCLs in unison. We have designed a linear quadratic regulator to enable the aggregate power demand to track reference signals. This suggests the derived aggregate response model could be used to allow load to track fluctuations in renewable generation. The analysis has been based on the assumptions that the TCL population is homogeneous and that the noise level is insignificant. Further studies are required to incorporate the effects of heterogeneity and noise into the model. Those extensions are important for determining the damping coefficient.

Similar analysis can be used to establish the aggregate characteristics of groups of plug-in electric vehicles, another candidate for compensating the variability in renewable generation.

ACKNOWLEDGEMENT

We thank Dr. Michael Chertkov of Los Alamos National Laboratory, USA for his support and useful insights throughout this work. We also thank Prof. Duncan Callaway for many helpful discussions.

REFERENCES

[1] S. Ihara and F.C. Schweppe, "Physically based modelling of cold load pickup", *IEEE Transactions on Power Apparatus and Systems*, 100(9):4142-4150, September 1981.

[2] C.Y. Chong and A.S. Debs, "Statistical synthesis of power system functional load models", *Proceedings of the 18th IEEE Conference on Decision and Control*, 264-269, December 1979.

[3] D.S. Callaway, "Tapping the energy storage potential in electric loads to deliver load following and regulation, with application to wind energy", *Energy Conversion and Management*, 50(5):1389-1400, May 2009.

[4] R. Malhamé and C.Y. Chong, "Electric load model synthesis by diffusion approximation of a high-order hybrid-state stochastic system", *IEEE Transactions on Automatic Control*, 30(9):854-860, September 1985.

[5] R.E. Mortensen and K.P. Haggerty, "A stochastic computer model for heating and cooling loads", *IEEE Transactions on Power Systems*, 3(3):1213-1219, August 1988.

[6] C. Uçak and R. Çağlar, "The effects of load parameter dispersion and direct load control actions on aggregated load", *POWERCON'98*, 1998.

[7] B.D.O. Anderson and J.B. Moore, "Optimal Control: Linear Quadratic Methods", *Prentice-Hall*, 1990.

A APPENDIX

This appendix provides an outline of the steps involved in deriving the expressions for $\mathbf{G}_a(s,\tau_a)$ and $\mathbf{G}_b(s,\tau_b)$. Derivation of the expressions for $\mathbf{G}_c(s,\tau_c)$ and $\mathbf{G}_d(s,\tau_d)$ is similar to that of $\mathbf{G}_a(s,\tau_a)$ and hence is not included.

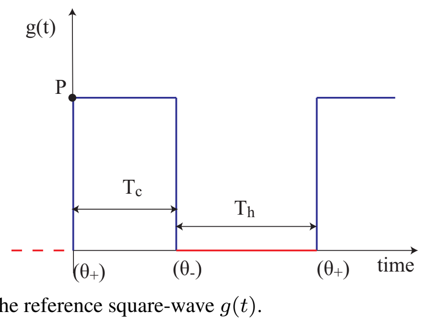

Figure 10: The reference square-wave $g(t)$.

A.1 Derivation of $\mathbf{G}_a(s,\tau_a)$

We note that the waveform $g_a(t,\tau_a)$ shown in Figure 6 is a time-shifted square-wave. Considering the waveform $g(t)$ in Figure 10, where $g(t)=0$ for $t<0$, we can express $g_a(t,\tau_a)$ as $g_a(t,\tau_a)=g(t-\tau_a)\mathbf{1}(t)$, where $\mathbf{1}(t)$ is the unit-step function, defined as

$$\mathbf{1}(t)=\begin{cases}1, & t\geq 0\\ 0, & t<0.\end{cases} \tag{20}$$

The Laplace transform of the square-wave $g(t)$ is $\mathbf{G}(s)=\frac{P(1-e^{-sT_c})}{s(1-e^{-s(T_c+T_h)})}$. Hence, the Laplace transform of $g_a(t,\tau_a)$ is

$$\begin{aligned}\mathbf{G}_a(s,\tau_a)&=\int_0^\infty g_a(t,\tau_a)e^{-st}dt\\ &=\int_0^\infty g(t-\tau_a)\mathbf{1}(t)e^{-st}dt\\ &=\int_0^\infty g(t-\tau_a)e^{-st}dt\\ &=\int_{-\tau_a}^\infty g(t^*)e^{-s(t^*+\tau_a)}dt^*\end{aligned}$$

where $t^*=t-\tau_a$. Therefore, because $g(t^*)=0, \forall t^*<0$,

$$\begin{aligned}\mathbf{G}_a(s,\tau_a)&=\int_0^\infty g(t^*)e^{-s(t^*+\tau_a)}dt^*\\ &=e^{-s\tau_a}\mathbf{G}(s).\end{aligned} \tag{21}$$

The expressions for $\mathbf{G}_c(s,\tau_c)$ and $\mathbf{G}_d(s,\tau_d)$ can be derived similarly.

A.2 Derivation of $\mathbf{G}_b(s,\tau_b)$

The square-wave $g_b(t,\tau_b)$ can be expressed as $g_b(t,\tau_b)=g(t+T_c-\tau_b)\mathbf{1}(t)$ and its Laplace transform as

$$\begin{aligned}\mathbf{G}_b(s,\tau_b)&=\int_0^\infty g_b(t,\tau_b)e^{-st}dt\\ &=\int_0^\infty g(t+T_c-\tau_b)\mathbf{1}(t)e^{-st}dt\\ &=\int_0^\infty g(t+T_c-\tau_b)e^{-st}dt\\ &=\int_{T_c-\tau_b}^\infty g(t^*)e^{-s(t^*-T_c+\tau_b)}dt^*\end{aligned}$$

where $t^*=t+T_c-\tau_b$. Therefore,

$$\begin{aligned}\mathbf{G}_b(s,\tau_b)=&e^{s(T_c-\tau_b)}\int_{T_c-\tau_b}^\infty g(t^*)e^{-st^*}dt^*\\ =&e^{s(T_c-\tau_b)}\int_0^\infty g(t^*)e^{-st^*}dt^*\\ &-e^{s(T_c-\tau_b)}\int_0^{T_c-\tau_b} g(t^*)e^{-st^*}dt^*\\ =&e^{s(T_c-\tau_b)}\mathbf{G}(s)\\ &-e^{s(T_c-\tau_b)}\int_0^{T_c-\tau_b} Pe^{-st^*}dt^*\\ =&e^{s(T_c-\tau_b)}\mathbf{G}(s)\\ &-e^{s(T_c-\tau_b)}P\frac{\left(1-e^{-s(T_c-\tau_b)}\right)}{s}\\ =&e^{s(T_c-\tau_b)}\mathbf{G}(s)-P\frac{\left(e^{s(T_c-\tau_b)}-1\right)}{s}.\end{aligned} \tag{22}$$